

First-principles density-functional calculations using localized spherical-wave basis sets

C. K. Gan, P. D. Haynes, and M. C. Payne¹

¹*Theory of Condensed Matter, Cavendish Laboratory,
Madingley Road, Cambridge CB3 0HE, United Kingdom*

We present a detailed study of the use of localized spherical-wave basis sets, first introduced in the context of linear-scaling, in first-principles density-functional calculations. Several parameters that control the completeness of this basis set are fully investigated on systems such as molecules and bulk crystalline silicon. We find that the results are in good agreement with those obtained using the extended plane-wave basis set. Since the spherical-wave basis set is accurate, easy to handle, relatively small, and can be systematically improved, we expect it to be of use in other applications.

PACS numbers: 71.15.Ap,71.15.Dx,71.15.Mb

I. INTRODUCTION

Localized basis sets such as Gaussians¹, truncated pseudo-atomic orbitals^{2,3}, real-space grids⁴⁻⁹, B-spline (or “blip”) functions¹⁰, and wavelets¹¹, have been used in first-principles calculations. Recently there has been a surge of activity to investigate linear-scaling methods¹² (where the computational effort and memory requirement scale linearly with the system size), all of which use localized basis sets in their implementations. One localized basis set that was introduced for linear-scaling methods, the spherical-wave basis set¹³, is interesting because while sharing some of the properties (such as the concept of energy cutoff) with the extended plane-wave basis set, it possesses other advantages such as each basis function being fully localized within a sphere. Even though it has been used to implement a linear-scaling method and tested against bulk crystalline silicon¹⁴, this basis set has not yet been fully investigated. This work serves to reveal the properties of this localized basis set using a matrix diagonalization approach, which frees us from having to consider other sources of error introduced by other cutoffs (such as the density-matrix spatial cutoff¹⁵⁻¹⁷). The completeness and appropriateness of this basis set are investigated in first-principles calculations within density-functional theory through applications to molecules and bulk crystalline silicon. The remainder of this work is organized as follows. Section II introduces the spherical-wave basis set. In section III, a brief description is given of the first-principles calculation within density-functional theory using the spherical-wave basis set. Section IV contains the results of calculations on different test systems, which are compared with those obtained using the same theory level and approximations, but with a plane-wave basis set¹⁸. Section V contains the summary and conclusions.

II. ORIGIN OF THE BASIS SET

The spherical-wave basis functions¹³ used in this work are eigenfunctions of the Helmholtz equation

$$(\nabla^2 + q^2)\chi(\mathbf{r}) = 0, \quad (1)$$

subject to boundary conditions such that the solutions $\chi(\mathbf{r})$ are nonvanishing only inside a sphere of radius R and vanishing whenever $|\mathbf{r}| \geq R$. The eigenfunctions are

$$\chi(r, \theta, \phi) = \begin{cases} j_\ell(q_{n\ell}r)Y_{\ell m}(\theta, \phi), & r < R, \\ 0, & r \geq R, \end{cases}$$

where (r, θ, ϕ) are spherical polar coordinates with origin at the center of the sphere, ℓ is a non-negative integer and m is an integer satisfying $-\ell \leq m \leq \ell$. $j_\ell(x)$ is the spherical Bessel function of order ℓ , and $Y_{\ell m}(\theta, \phi)$ is a spherical harmonic. The eigenvalue $q_{n\ell}$ is determined from the n th zero of $j_\ell(x)$ where

$$j_\ell(q_{n\ell}R) = 0. \quad (2)$$

We note that each eigenfunction in Eq. (2) has an energy of $\hbar^2 q_{n\ell}^2 / (2m_e)$, hence it is possible to use the concept of cutoff energy to restrict the number of $q_{n\ell}$ in the expansion of a wavefunction.

The real spherical-wave basis functions used in this work are

$$\chi_{\alpha, n\ell m}(\mathbf{r}) = \begin{cases} j_\ell(q_{\alpha, n\ell}|\mathbf{r} - \mathbf{R}_\alpha|)\bar{Y}_{\ell m}(\Omega_{\mathbf{r} - \mathbf{R}_\alpha}), & |\mathbf{r} - \mathbf{R}_\alpha| < r_\alpha, \\ 0, & |\mathbf{r} - \mathbf{R}_\alpha| \geq r_\alpha, \end{cases}$$

where α signifies a *basis sphere* with radius r_α and centered at \mathbf{R}_α . $\bar{Y}_{\ell m}(\theta, \phi)$ are the real linear combinations of the spherical harmonics. By construction, all basis functions within a basis sphere are orthogonal to one another. In general, more than one basis sphere is needed to expand a wavefunction

$$\psi(\mathbf{r}) = \sum_{\alpha, n\ell m} c_{\alpha, n\ell m} \chi_{\alpha, n\ell m}(\mathbf{r}), \quad (3)$$

where $c_{\alpha, n\ell m}$ are the associated coefficients. For most systems tested in this work, we have used one basis sphere per atom, where the basis spheres are centered on the atoms. For some systems we have increased the number of basis spheres by placing basis spheres between the atoms. In principle it is possible to use two or more basis spheres of different radii centered on the same atom, but this arrangement has not been studied in this work. We note that even though the basis functions belonging to

different basis spheres are generally nonorthogonal, one of the main advantages of this basis set is that it is possible to analytically evaluate¹³ the overlap matrix elements

$$S_{\alpha,n\ell m;\beta,n'\ell'm'} = \int d\mathbf{r} \chi_{\alpha,n\ell m}(\mathbf{r})\chi_{\beta,n'\ell'm'}(\mathbf{r}), \quad (4)$$

and kinetic energy matrix elements

$$T_{\alpha,n\ell m;\beta,n'\ell'm'} = -\frac{\hbar^2}{2m_e} \int d\mathbf{r} \chi_{\alpha,n\ell m}(\mathbf{r})\nabla^2\chi_{\beta,n'\ell'm'}(\mathbf{r}). \quad (5)$$

We also note that the matrix elements for the nonlocal pseudopotentials in the Kleinman-Bylander¹⁹ form can also be evaluated analytically by first expanding the projectors in the spherical-wave basis set.

III. DENSITY-FUNCTIONAL CALCULATIONS

The Kohn-Sham (KS) equation for an M -electron system is^{20,21}

$$\hat{H}\psi_m(\mathbf{r}) = \left[-\frac{\hbar^2}{2m_e}\nabla^2 + V_{\text{eff}}(\mathbf{r}) \right] \psi_m(\mathbf{r}) = \varepsilon_m\psi_m(\mathbf{r}), \quad (6)$$

where $\{\psi_m(\mathbf{r})\}$ are the KS eigenfunctions with corresponding eigenvalues $\{\varepsilon_m\}$. The effective potential $V_{\text{eff}}(\mathbf{r})$ consists of the classical electrostatic potential, the ionic potential due to the nuclei and the exchange-correlation potential. The effective potential depends on the electron density, $\rho(\mathbf{r})$, which is formed from the M lowest eigenstates

$$\rho(\mathbf{r}) = \sum_{m=1}^M |\psi_m(\mathbf{r})|^2. \quad (7)$$

We use the real spherical-wave basis set $\{\chi_\nu(\mathbf{r})\}$ to expand the n -th KS eigenstate

$$\psi_n(\mathbf{r}) = \sum_{\nu} x_n^{\nu} \chi_{\nu}(\mathbf{r}), \quad (8)$$

where ν is a collective label for $(\alpha, n\ell m)$ in Eq. (3). Substituting Eq. (8) into Eq. (6), and taking inner products with the $\{\chi_{\mu}(\mathbf{r})\}$, we obtain the generalized eigenvalue problem

$$\sum_{\nu} (H_{\mu\nu} - \varepsilon_n S_{\mu\nu}) x_n^{\nu} = 0, \quad (9)$$

where the overlap matrix is given by

$$S_{\mu\nu} = \int d\mathbf{r} \chi_{\mu}(\mathbf{r})\chi_{\nu}(\mathbf{r}), \quad (10)$$

and the Hamiltonian matrix is given by

$$H_{\mu\nu} = \int d\mathbf{r} \chi_{\mu}(\mathbf{r})\hat{H}\chi_{\nu}(\mathbf{r}). \quad (11)$$

It should be emphasized that when a large system is studied, S and H will be sparse. In this case it is more efficient to use an iterative method based on preconditioned conjugate gradient minimization²² to find the lowest few eigenvalues and corresponding eigenvectors of Eq. (9) than to use a direct matrix diagonalization method^{23,24} in which all eigenvalue-eigenvector pairs are found.

The completeness of the basis set depends on several parameters such as the radius of the basis sphere, R ; the maximum angular momentum component, ℓ_{max} ; and the number of $q_{n\ell}$ values for each angular momentum component, which we will take here to be the same for all ℓ and is denoted by n_q . The number of basis functions in a basis sphere is $(\ell_{\text{max}} + 1)^2 n_q$. For a fixed number of n_q , we note that the number of basis functions increases very rapidly with respect to ℓ_{max} . However, we will demonstrate that most physical properties can be deduced using only a small ℓ_{max} , which is typically 2. The cutoff energy E_c for a basis sphere is roughly given by

$$E_c = \frac{\hbar^2}{2m_e} \left(\frac{n_q\pi}{R} \right)^2. \quad (12)$$

Periodicity of the system under study is assumed and the Γ point only is used for the Brillouin zone sampling. We have used the local density approximation (LDA) for the exchange and correlation term. Norm-conserving Troullier-Martins²⁵ pseudopotentials in the Kleinman-Bylander¹⁹ form are used.

IV. RESULTS OF THE CALCULATIONS

In this section we present and discuss the results obtained from density-functional calculations using the spherical-wave basis set. We study the convergence of the total energy as a function of the cutoff energy, E_c ; the radii of the basis spheres, R ; the maximum angular momentum component, ℓ_{max} ; and the number of basis spheres, N_{bs} . Physical properties are deduced from total energy calculations on the systems. For molecules, we calculate the equilibrium bond lengths and force constants. For bulk crystalline silicon, we calculate the equilibrium lattice parameter and bulk modulus. These results are compared with those obtained using a plane-wave code¹⁸, and from experiment²⁶.

In Fig. 1 we plot the total energy of the chlorine molecule with a bond length of 1.6 Å as a function of cutoff energy E_c and basis sphere radius R . The figure shows that the total energy decreases rapidly as the cutoff energy and the basis sphere radius are increased, which is to be expected from the additional variational freedom that is introduced. Convergence in the total energy is achieved for cutoff energies above 800 eV.

Fig. 2 shows that the rate of convergence of the total energy with respect to the cutoff energy is the same for both the localized spherical-wave and extended plane-wave basis sets. This confirms that the energy cutoff

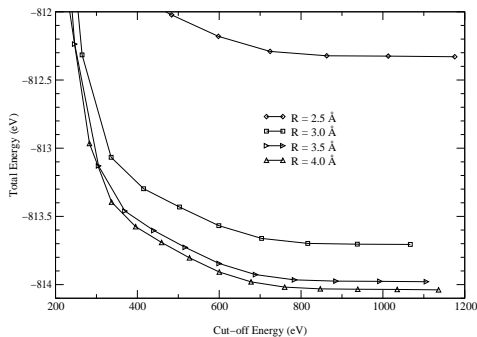


FIG. 1. Total energy of the chlorine molecule with a bond length of 1.6 Å. Two basis spheres of radius R centered on the atoms are used. The cubic simulation cell has sides of length 12 Å. $\ell_{\max} = 2$.

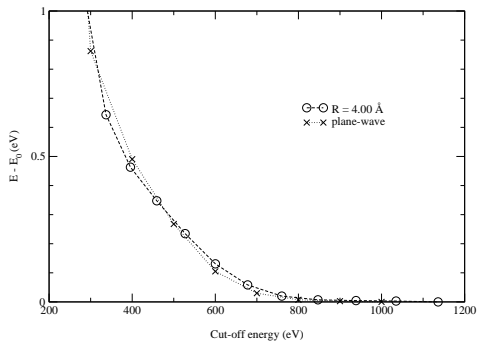


FIG. 2. Nature of the convergence of the total energy of the chlorine molecule with a bond length of 1.6 Å. The data for the spherical-wave basis set are taken from Fig. 1. The respective converged total energies E_0 are subtracted from the total energy E in each case.

concept can be equally applied in the spherical-wave basis set.

Using an energy cutoff above 900 eV, we calculate the total energy of the chlorine molecule for a variety of bond lengths as a function of the basis sphere radius R . Fig. 3 shows that the total energy converges exponentially with respect to R . We also note that the total energy converges slightly faster with respect to R for molecules with smaller bond lengths. This reflects the fact that for a given R , the basis set is more complete for a smaller molecule than a larger one because the basis spheres are closer to one another in the smaller molecule.

Since the total energy also depends on other parameters such as ℓ_{\max} and the number of basis spheres N_{bs} , we have performed calculations on the chlorine molecule with a bond length of 2.4 Å. The results in Fig. 4 show the convergence of the total energy of the system as a function of ℓ_{\max} for different basis-sphere radii R and numbers of basis spheres N_{bs} . The rapid convergence of the total energy with respect to ℓ_{\max} is evident from the figure. We note that the “best” result obtained from the spherical-wave calculation with $N_{\text{bs}} = 2$, $R = 4.50$ Å, and $\ell_{\max} = 3$ gives a total energy of -815.958 eV,

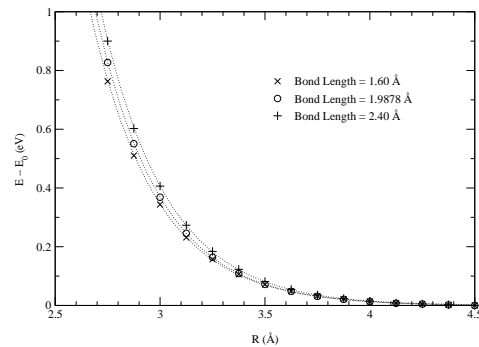


FIG. 3. Convergence of the total energy of the chlorine molecule for a variety of bond lengths. The respective converged total energies E_0 are subtracted from the total energy E in each case. Two basis spheres of radius R centered on the atoms are used. The dotted curves are exponential fits to the data.

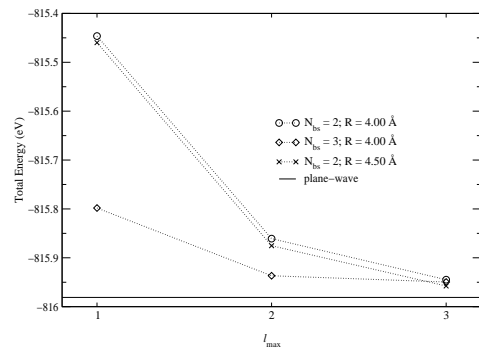


FIG. 4. Total energy of the chlorine molecule with a bond length of 2.4 Å as a function of the maximum angular momentum component ℓ_{\max} for different basis-sphere radii R and numbers of basis spheres N_{bs} . For the three-basis-sphere calculations, two basis spheres are centered on the atoms and a third basis sphere is centered between the atoms. For each spherical-wave calculation, we have used a value of n_q which is the smallest integer such that the cutoff energy exceeds 900 eV. The horizontal solid line corresponds to the total energy obtained from the plane-wave calculation with a cutoff energy of 900 eV.

which lies 0.023 eV above the plane-wave total energy of -815.981 eV. This difference, which is due to the incompleteness of the spherical-wave basis set, could be reduced further by increasing the basis-sphere radius R and ℓ_{\max} . However, we are content with this accuracy because the error due to the incompleteness of the spherical-wave basis set is only about 3×10^{-5} of the total energy obtained from the plane-wave calculation. The number of spherical-wave basis functions in this case is only 672, which is a small fraction (0.6%) of 112452, the number of plane waves.

To study the effect of N_{bs} , ℓ_{\max} and R on the calculated physical properties such as the equilibrium bond length r_e and force constant f , we perform a series of calculations on the chlorine molecule for a range of bond

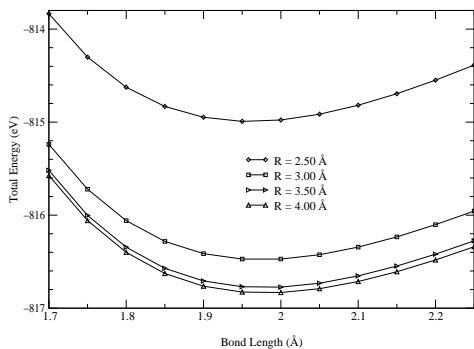


FIG. 5. Total energy of the chlorine molecule as a function of the bond length. Two basis spheres of the same radius R centered on the atoms are used. $\ell_{\max} = 2$.

$R(\text{\AA})$	$N_{\text{bs}} = 2$				$N_{\text{bs}} = 3$			
	$r_e(\text{\AA})$	$\delta r_e(\%)$	$f(\frac{\text{N}}{\text{cm}})$	$\delta f(\%)$	$r_e(\text{\AA})$	$\delta r_e(\%)$	$f(\frac{\text{N}}{\text{cm}})$	$\delta f(\%)$
2.00	1.8941	-3.66	5.276	39.2	1.9158	-2.56	4.591	21.1
2.50	1.9609	-0.26	3.959	4.5	1.9537	-0.63	4.017	6.0
3.00	1.9733	0.37	3.754	-0.9	1.9636	-0.13	3.849	1.6
3.50	1.9769	0.55	3.694	-2.5	1.9658	-0.02	3.802	0.3
4.00	1.9777	0.59	3.673	-3.1	1.9663	0.01	3.789	0.0
4.50	1.9778	0.60	3.670	-3.2	1.9663	0.01	3.786	-0.1

TABLE I. Results for the equilibrium bond length r_e and force constant f of the chlorine molecule with $\ell_{\max} = 2$. The meanings of R and N_{bs} are explained in the caption of Table II.

lengths from 1.70 Å to 2.25 Å. A typical result is shown in Fig. 5. The results of the calculations of r_e and f with $\ell_{\max} = 1, 2$, and 3 are displayed in Tables II, I, and III, respectively. The errors in r_e and f displayed in the columns headed under δr_e and δf are deduced from the results of the plane-wave calculations.

In Table II, the values of r_e and f converge rapidly with respect to R . However, the results with two basis spheres and $\ell_{\max} = 1$ shows that the converged results contain unacceptably large systematic errors. The inclusion of a third sphere reduces the errors significantly because the bonding region between the atoms is described better by the third sphere. The results show it is impossible to improve the results simply by enlarging R when $\ell_{\max} = 1$ is used.

We repeat the calculations for r_e and f with $\ell_{\max} = 2$, for which the results are presented in Table I. The converged results with $N_{\text{bs}} = 2$ and $\ell_{\max} = 2$ are better than the converged results with $N_{\text{bs}} = 3$ and $\ell_{\max} = 1$, which indicates the importance of ℓ_{\max} over N_{bs} for the “minimal basis set” calculations. With $\ell_{\max} = 2$ and $N_{\text{bs}} = 2$, the error of the converged results for r_e and f are -0.50% and 13.6% compared to the experimental values, respectively. These accuracies are acceptable within the LDA.

Finally in Table III, we present the values of r_e and f using two basis spheres centered on the atoms $\ell_{\max} = 3$. As expected, the converged values of r_e and f agree very

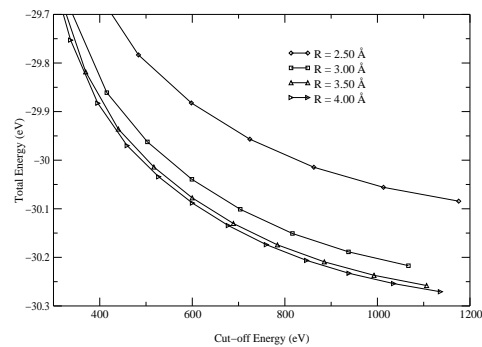


FIG. 6. Total energy of the hydrogen molecule with a bond length of 1.0 Å. Two basis spheres of the same radius R centered on the atoms are used. $\ell_{\max} = 2$. The cubic simulation cell has sides of length 12 Å.

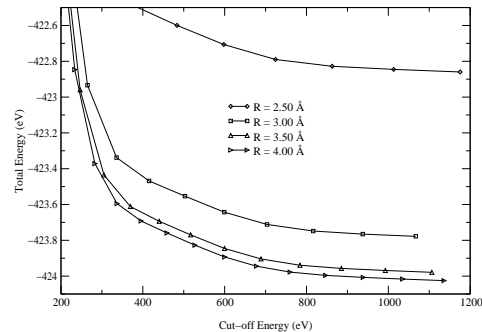


FIG. 7. Total energy of the hydrogen chloride molecule with a bond length of 1.6 Å as a function of the cutoff energy and the basis sphere radius R . Two basis spheres of the same radius R centered on the atoms are used. The cubic simulation cell has sides of length 12 Å. $\ell_{\max} = 2$.

well with the plane-wave results. We note that calculations with $\ell_{\max} = 3$ are expensive, since the number of basis functions is almost double that for $\ell_{\max} = 2$.

Next we calculate the total energy of hydrogen molecule with a bond length of 1.0 Å as a function of the cutoff energy E_c , and the basis sphere radius R , for which the results are displayed in Fig. 6. The total energy converges rather slowly with respect to the cutoff energy because a bare Coulomb potential due to the hydrogen atom is used. Such behavior is also observed in the plane-wave calculations. However, the convergence of energy differences is achieved when the cutoff energy exceeds 800 eV.

We perform a series of total energy calculations on the hydrogen molecule for a range of bond lengths to determine the values of r_e and f . The results are tabulated in Table IV and show that we can use a value of R as small as 3.00 Å to obtain an accuracy of less than 1% in r_e and f with only two basis spheres. This should be contrasted with the case of the chlorine molecule where with $N_{\text{bs}} = 2$, $\ell_{\max} = 2$, and $R = 3.00$ Å, the values of r_e and f agree only fortuitously with the plane-wave results.

We can explain why, to obtain the same accuracy, the chlorine molecule requires a larger R than the hydrogen molecule. The equilibrium bond length of the hydrogen molecule (which is about 0.74 Å) is smaller than the equilibrium bond length of the chlorine molecule (which is about 1.99 Å). The bonding region between the hydrogen atoms is thus described better by the basis functions because the basis spheres are closer to one another. The hydrogen molecule is also “smaller” (in the sense of the extent of the charge distribution) than the chlorine molecule.

In Fig. 7 we show the total energy of the hydrogen chloride molecule with a bond length of 1.60 Å as a function of the cutoff energy and the radius of the basis sphere. The energy differences converge when the cutoff energy exceeds 800 eV. Calculations are performed to obtain r_e and f , and the results are tabulated in Table V.

We repeat the r_e and f calculations for the hydrogen chloride molecule, where the radius of the basis sphere centered on the chlorine atom is fixed at 4.00 Å but the radius of the basis sphere centered on the hydrogen atom is varied. The results are presented in Table VI, which shows that we can use a smaller basis sphere of a radius of 2.0 Å centered on the hydrogen atom to obtain an accuracy of less than 1%. It is thus possible to use different basis spheres depending on the atomic species, which is important because this can reduce the computation time significantly.

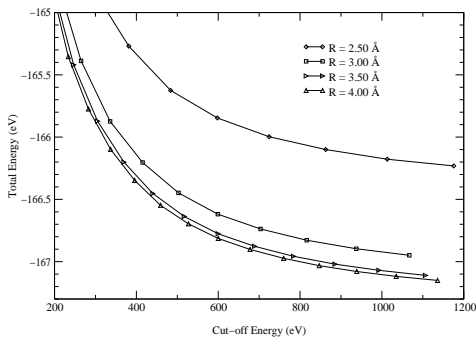


FIG. 8. Total energy of the silane molecule with the Si-H bond length of 1.83 Å. Five basis spheres of the same radius R centered on the atoms are used. The cubic simulation cell has a side length of 12 Å. $\ell_{\max} = 2$.

Fig. 8 shows the total energy of the silane molecule with a Si-H bond length of 1.83 Å, as a function of E_c and R . Total energy differences converge for cutoff energies above 800 eV. The results of the calculations of r_e and f (for the breathing mode) are summarized in Table VII. We find that the accuracy is acceptable when $R = 3.00$ Å.

We repeat the r_e and f calculations on the silane molecule with the radius of the basis sphere centered on the silicon atom fixed at 4.00 Å, but with the radius R of the basis spheres centered on the hydrogen atoms varied. The results in Table VIII show that an accuracy of 1% can be achieved by using $R = 3.00$ Å, which is 1 Å larger than the basis spheres centered on the hydrogen

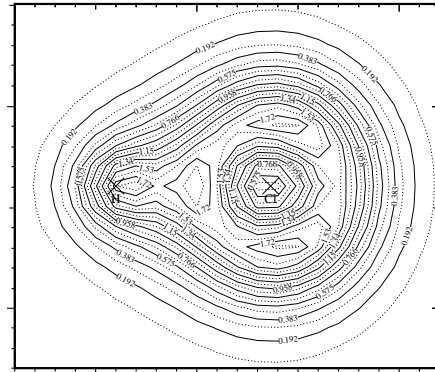


FIG. 9. Electronic densities (in units of electrons/Å³) on the plane containing atoms of the hydrogen chloride molecule with a bond length of 1.2746 Å. The locations of the atoms are marked by crosses.

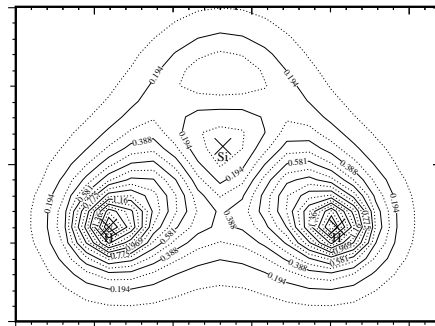


FIG. 10. Electronic densities (in units of electrons/Å³) on the plane containing three atoms of the tetrahedral silane molecule with bond lengths of 1.4798 Å. The locations of the atoms are marked by crosses.

atom in the hydrogen chloride molecule calculation (c.f. Table VI).

From the pseudo-charge density of the hydrogen chloride molecule (Fig. 9), we observe that the valence electrons are concentrated towards the chlorine atom, as expected from the relative electronegativities of hydrogen and chlorine. This enables us to use a smaller basis sphere centered on the hydrogen atom to obtain accurate results. However, from the pseudo-charge density of the silane (Fig. 10), we observe substantial charge density around the hydrogen atoms, reflecting the fact that hydrogen is more electronegative than silicon. Hence for the silane molecule calculations, the radius of the basis spheres centered on the hydrogen atoms need to be larger than that for hydrogen chloride. These observations lead to the conclusion that the relative electronegativities of neighboring atoms in a calculation should be taken into account when choosing basis sphere radii.

We have chosen bulk crystalline silicon to test the performance of the basis set on an extended system. Fig. 11 shows the total energy per atom for a 64-atom cell of sil-

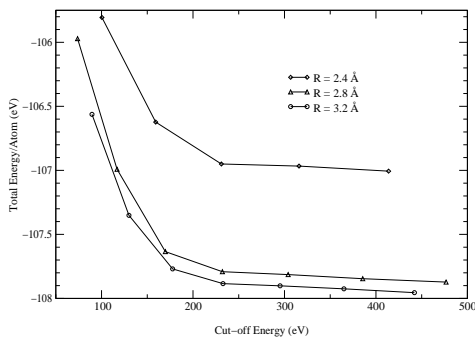


FIG. 11. Total energy of a 64-atom cell of bulk crystalline silicon with a lattice parameter of 5.43 Å and $\ell_{\max} = 2$. 64 basis spheres of the same radius R centered on the atoms are used.

icon with a lattice parameter of 5.43 Å as a function of the cutoff energy and R . The total energy converges at a cutoff energy of about 250 eV. The rapid convergence of the total energy with respect to R is evident from the figure.

To determine the equilibrium lattice parameter, a , and the bulk modulus, B , we perform a series of calculations on the bulk silicon system for a range of lattice parameters from 5.31 Å to 5.51 Å. The results of the calculations with $\ell_{\max} = 1$ and 2 are tabulated in Tables IX and X, respectively. It is found that even with $\ell_{\max} = 1$, the results with $R = 3.20$ Å agree quite well with the plane-wave and experiment results. The calculations with $\ell_{\max} = 2$ improve the results slightly. The reason why $\ell_{\max} = 1$ calculations give rather good results is because silicon atoms mix the s and p states to form four sp^3 orbitals which are obviously well-described by a basis set with $\ell_{\max} = 1$.

Finally we present Table XI which shows the numbers of basis functions for the spherical-wave and plane-wave basis set calculations. Since in general the number of spherical-wave basis functions is very small for molecules compared to that of plane-wave basis functions, we conclude that spherical-wave basis sets can be used to study molecules and possibly clusters with high efficiency.

V. CONCLUSIONS

Through detailed calculations on molecules and bulk crystalline silicon, we find that the total energy and phys-

ical properties can be accurately deduced from density-functional calculations using localized spherical-wave basis sets. We find that for most purposes, the choice of $\ell_{\max} = 2$ and atom-centered basis spheres is sufficient to obtain an accuracy which is excellent compared to those obtained using the extended plane-wave basis set.

The dependence of the total energy on the cutoff energy of the localized basis set is found to be rather similar to that of the extended plane-wave basis set. We also find that the results converge exponentially with respect to the basis sphere radius R . The angular incompleteness can be improved either by increasing ℓ_{\max} , or by introducing additional basis spheres at strategic locations (such as at the middle of a bond).

We find that the radii of the basis spheres depend on the bond lengths. A large bond length usually means large basis spheres are to be used. We find that it is possible to use different radii for the basis spheres depending on the relative electronegativities of the atomic species. Usually we need to use basis spheres with larger radii for atoms that are more electronegative than other atoms in a calculation.

For the bulk silicon case, the accuracy of the results obtained using $\ell_{\max} = 1$ is marginally acceptable, which is a consequence of the sp^3 hybridization.

Finally, we note that one of the main advantages of this basis set is that the accuracy of the results can be systematically improved. It would be interesting to explore the possibility of using two or more basis spheres of different radii centered on an atom so that a lower cutoff energy for the larger basis spheres might be used.

ACKNOWLEDGEMENT

C.K.G. acknowledges financial support from the Cambridge Commonwealth Trust and from St. John's College, Cambridge. P.D.H. acknowledges the support of a Research Fellowship from Magdalene College, Cambridge.

¹ S. F. Boys, Proc. R. Soc. London, Ser. A **200**, 542 (1950).

² O. F. Sankey and D. J. Niklewski, Phys. Rev. B **40**, 3979 (1989).

³ E. Artacho *et al.*, Phys. Status Solidi B **215**, 809 (1999).

⁴ J. R. Chelikowsky, N. Troullier, and Y. Saad, Phys. Rev. Lett. **72**, 1240 (1994).

⁵ J. R. Chelikowsky, N. Troullier, K. Wu, and Y. Saad, Phys. Rev. B **50**, 11355 (1994).

⁶ N. A. Modine, G. Zumbach, and E. Kaxiras, Phys. Rev. B **55**, 10289 (1997).

⁷ J. Bernholc *et al.*, Int. J. Quantum Chem. **65**, 531 (1997).

⁸ J.-L. Fattebert and J. Bernholc, Phys. Rev. B **62**, 1713 (2000).

- ⁹ T. L. Beck, *Rev. Mod. Phys.* **72**, 1041 (2000).
- ¹⁰ E. Hernández, M. J. Gillan, and C. M. Goringe, *Phys. Rev. B* **55**, 13485 (1997).
- ¹¹ T. A. Arias, *Rev. Mod. Phys.* **71**, 267 (1999).
- ¹² S. Goedecker, *Rev. Mod. Phys.* **71**, 1085 (1999).
- ¹³ P. D. Haynes and M. C. Payne, *Comput. Phys. Commun.* **102**, 17 (1997).
- ¹⁴ P. D. Haynes and M. C. Payne, *Phys. Rev. B* **59**, 12173 (1999).
- ¹⁵ X.-P. Li, R. W. Nunes, and D. Vanderbilt, *Phys. Rev. B* **47**, 10891 (1993).
- ¹⁶ E. Hernández, M. J. Gillan, and C. M. Goringe, *Phys. Rev. B* **53**, 7147 (1996).
- ¹⁷ P. D. Haynes and M. C. Payne, *Solid State Commun.* **108**, 737 (1998).
- ¹⁸ M. C. Payne *et al.*, *Rev. Mod. Phys.* **64**, 1045 (1992).
- ¹⁹ L. Kleinman and D. M. Bylander, *Phys. Rev. Lett.* **48**, 1425 (1982).
- ²⁰ P. Hohenberg and W. Kohn, *Phys. Rev.* **136**, 864B (1964).
- ²¹ W. Kohn and L. J. Sham, *Phys. Rev.* **140**, 1133A (1965).
- ²² C. K. Gan, P. D. Haynes, and M. C. Payne, *Comput. Phys. Commun.* **134**, 33 (2001).
- ²³ G. H. Golub and C. F. van Loan, *Matrix Computations*, 3rd ed. (Johns Hopkins University Press, Baltimore, 1996).
- ²⁴ W. Press, B. P. Flannery, S. A. Teukolsky, and W. T. Vetterling, *Numerical Recipes, the Art of Scientific Computing* (Cambridge University Press, Cambridge, England, 1986).
- ²⁵ N. Troullier and J. L. Martins, *Phys. Rev. B* **43**, 1993 (1991).
- ²⁶ *CRC Handbook of Chemistry and Physics: a Ready-Reference Book of Chemical and Physical Data*, 76th ed., edited by D. R. Lide and H. P. R. Frederikse (CRC Press, London, 1995).

$R(\text{\AA})$	$N_{\text{bs}} = 2$				$N_{\text{bs}} = 3$			
	$r_e(\text{\AA})$	$\delta r_e(\%)$	$f(\frac{\text{N}}{\text{cm}})$	$\delta f(\%)$	$r_e(\text{\AA})$	$\delta r_e(\%)$	$f(\frac{\text{N}}{\text{cm}})$	$\delta f(\%)$
2.00	2.0214	2.81	4.880	28.8	1.9565	-0.49	4.492	18.5
2.50	2.1240	8.03	2.542	-32.9	1.9988	1.66	3.747	-1.1
3.00	2.1536	9.54	1.874	-50.6	2.0098	2.22	3.557	-6.1
3.50	2.1595	9.84	1.772	-53.2	2.0123	2.35	3.496	-7.8
4.00	2.1623	9.98	1.703	-55.1	2.0127	2.37	3.484	-8.1
4.50	2.1625	9.99	1.701	-55.1	2.0128	2.38	3.481	-8.2

TABLE II. Results for the equilibrium bond length r_e and force constant f of the chlorine molecule with $\ell_{\text{max}} = 1$. When $N_{\text{bs}} = 2$, two basis spheres of the same radius R centered on the atoms are used. When $N_{\text{bs}} = 3$, three basis spheres of the same radius R are used, the third basis sphere being centered between the atoms. The experimental values for r_e and f are 1.9878 Å and 3.23 N/cm, respectively. The plane-wave calculations give values of 1.9661 Å and 3.790 N/cm, respectively, where we have used the same pseudopotentials, Brillouin zone sampling, and cutoff energy.

$R(\text{\AA})$	$r_e(\text{\AA})$	$\delta r_e(\%)$	$f(\frac{\text{N}}{\text{cm}})$	$\delta f(\%)$
2.00	1.8833	-4.21	5.212	37.5
2.50	1.9481	-0.92	4.128	8.9
3.00	1.9636	-0.13	3.860	1.8
3.50	1.9668	0.04	3.792	0.1
4.00	1.9674	0.07	3.777	-0.3
4.50	1.9675	0.07	3.773	-0.4

TABLE III. Results for the equilibrium bond length r_e and force constant f of the chlorine molecule with $\ell_{\text{max}} = 3$.

$R(\text{\AA})$	$N_{\text{bs}} = 2$				$N_{\text{bs}} = 3$			
	$r_e(\text{\AA})$	$\delta r_e(\%)$	$f(\frac{\text{N}}{\text{cm}})$	$\delta f(\%)$	$r_e(\text{\AA})$	$\delta r_e(\%)$	$f(\frac{\text{N}}{\text{cm}})$	$\delta f(\%)$
2.00	0.7476	-3.05	5.998	15.4	0.7503	-2.70	5.865	12.9
2.50	0.7643	-0.88	5.420	4.3	0.7668	-0.56	5.232	0.7
3.00	0.7695	-0.21	5.237	0.8	0.7712	0.01	5.198	0.0
3.50	0.7709	-0.03	5.193	-0.1				
4.00	0.7710	-0.01	5.178	-0.4				

TABLE IV. Results for the equilibrium bond length r_e and force constant f of the hydrogen molecule with $\ell_{\text{max}} = 2$. The meanings of R and N_{bs} are explained in the caption of Table II. Cut-off energies above 1000 eV are used. The experimental values for r_e and f are 0.7414 Å and 5.75 N/cm respectively. The equivalent plane-wave calculations give values of 0.7711 Å and 5.197 N/cm, respectively.

$R(\text{\AA})$	$N_{\text{bs}} = 2$				$N_{\text{bs}} = 3$			
	$r_e(\text{\AA})$	$\delta r_e(\%)$	$f(\frac{\text{N}}{\text{cm}})$	$\delta f(\%)$	$r_e(\text{\AA})$	$\delta r_e(\%)$	$f(\frac{\text{N}}{\text{cm}})$	$\delta f(\%)$
2.00	1.2601	-2.68	6.351	16.4	1.2712	-1.82	6.030	10.5
2.50	1.2862	-0.66	5.683	4.1	1.2885	-0.49	5.605	2.7
3.00	1.2926	-0.17	5.518	1.1	1.2933	-0.12	5.489	0.6
3.50	1.2936	-0.09	5.475	0.3	1.2941	-0.05	5.461	0.1
4.00	1.2942	-0.05	5.466	0.1	1.2946	-0.02	5.452	-0.1
4.50	1.2945	-0.02	5.464	0.1	1.2948	0.00	5.450	-0.1

TABLE V. Results for the equilibrium bond length r_e and force constant f of the hydrogen chloride molecule with $\ell_{\text{max}} = 2$. The meanings of R and N_{bs} are explained in the caption of Table II. For the hydrogen chloride molecule, the experimental values for r_e and f are 1.2746 \AA and 5.16 N/cm, respectively. The equivalent plane-wave calculations give values of 1.2948 \AA and 5.458 N/cm.

$R(\text{\AA})$	$r_e(\text{\AA})$	$\delta r_e(\%)$	$f(\frac{\text{N}}{\text{cm}})$	$\delta f(\%)$
2.00	1.2928	-0.15	5.508	0.9
2.50	1.2937	-0.08	5.488	0.5
3.00	1.2943	-0.04	5.472	0.3
3.50	1.2939	-0.07	5.468	0.2
4.00	1.2942	-0.05	5.466	0.1

TABLE VI. Results for r_e and f of the hydrogen chloride molecule. Two basis spheres are used. The radius of the basis sphere centered on the chlorine atom is fixed at 4.00 \AA but the radius R of the basis sphere centered on the hydrogen atom is varied.

$R(\text{\AA})$	$r_e(\text{\AA})$	$\delta r_e(\%)$	$f(\frac{\text{N}}{\text{cm}})$	$\delta f(\%)$
2.00	1.4402	-3.41	14.640	28.6
2.50	1.4811	-0.66	12.010	5.5
3.00	1.4893	-0.11	11.523	1.3
3.50	1.4906	-0.03	11.415	0.3
4.00	1.4912	0.01	11.382	0.0
4.50	1.4914	0.03	11.379	0.0

TABLE VII. Results for r_e and f of the silane molecule. Five basis spheres of the same radius R centered on the atoms are used. The cubic simulation cell has sides of length 12 \AA . $\ell_{\text{max}} = 2$. The experimental value of r_e is 1.4798 \AA , while the equivalent plane-wave calculations give the values of 1.4910 \AA and 11.38 N/cm for r_e and f , respectively.

$R(\text{\AA})$	$r_e(\text{\AA})$	$\delta r_e(\%)$	$f(\frac{\text{N}}{\text{cm}})$	$\delta f(\%)$
2.00	1.4851	-0.40	11.847	4.1
2.50	1.4856	-0.36	11.948	5.0
3.00	1.4902	-0.05	11.438	0.5
3.50	1.4906	-0.03	11.419	0.3
4.00	1.4912	0.01	11.382	0.0

TABLE VIII. Results for r_e and f of the silane molecule. Five basis spheres centered on the atoms are used. The radius of the basis sphere centered on the silicon atom is fixed at 4.00 \AA but the radius R of basis spheres centered on the hydrogen atoms is varied.

$R(\text{\AA})$	$a(\text{\AA})$	$\delta a(\%)$	$B(\text{GPa})$	$\delta B(\%)$
2.60	5.353	-0.78	139.1	50.7
2.80	5.413	0.33	104.5	13.2
3.00	5.445	0.93	97.0	5.1
3.20	5.453	1.08	89.8	-2.7

TABLE IX. Results for the equilibrium lattice parameter a and bulk modulus B of the 64-atom bulk crystalline silicon, with $\ell_{\max} = 1$. 64 basis spheres of the same radius R centered on the atoms are used. The experimental values for a and B are 5.43 Å and 100.0 GPa, respectively. The plane-wave calculations, with a cutoff energy of 250 eV, give the results of 5.395 Å and 92.3 GPa, respectively.

$R(\text{\AA})$	$a(\text{\AA})$	$\delta a(\%)$	$B(\text{GPa})$	$\delta B(\%)$
2.60	5.310	-1.58	238.0	157.9
2.80	5.353	-0.78	129.8	40.6
3.00	5.377	-0.33	111.4	20.7
3.20	5.385	-0.19	96.2	4.2

TABLE X. Results for the equilibrium lattice parameter a and bulk modulus B of the 64-atom bulk crystalline silicon, with $\ell_{\max} = 2$. 64 basis spheres of the same radius R centered on the atoms are used.

System	$E_c(\text{eV})$	N_{SW}	N_{PW}
Chlorine molecule	800	234	88663
Hydrogen molecule	1000	270	124097
HCl molecule	800	288	88663
Silane molecule	800	720	88663
Bulk silicon	250	4608	10827

TABLE XI. Numbers of the basis functions required so that the agreement between the results for r_e and f (for molecules); and a and B (for bulk silicon) from the spherical-wave and plane-wave basis set calculations is less than 1%. The numbers of the spherical-wave and plane-wave basis functions are denoted by N_{SW} and N_{PW} , respectively. For the spherical-wave basis set calculations, the choice of atom-centered and $\ell_{\max} = 2$ is used. E_c is the cutoff energy.